COMPARISON OF THERMAL FATIGUE BEHAVIOUR OF SILICA AND ALUMINA FOR INDUCTION FURNACE WALL

Nirajkumar Mehta[1], Dipesh Shukla[2]

[1]Associate Professor, ITM (SLS) Baroda University, Vadodara, Gujarat, India
[2]Ex-Director, Amity University, Jaipur, Rajasthan, India

ABSTRACT:

Furnaces are most commonly used for melting of ferrous metals and its alloy materials. Induction furnaces use electrical power so that they are more advantageous as no fuel is required. It is a very critical problem to find life span of induction melting furnace wall under thermal fatigue conditions. The life cycle of induction furnace refractory wall is a variable as minor variation is always present due to effect of skill of workers and many other factors. The heating cooling cycle of induction furnace wall will result in increasing and decreasing thermal stresses. The thermal fatigue behaviour of induction furnace wall is compared in this paper for silica ramming mass and alumina ramming mass. We have used two different methods including experimental investigation and numerical analysis.

Keywords: - *Induction Furnace, Heat Transfer, Silica Ramming Mass, Alumina Ramming Mass, Thermal Fatigue*

NOMENCLATURE

k	Thermal conductivity
ρ	Density
C	Specific heat
T	Temperature
Δt	Time interval
ha	Convective co-efficient of atmosphere
ho	Convective co-efficient of coolant
hi	Convective co-efficient of molten metal
T_x^i	Temperature of node x at i instantaneous time
S	Stress
Δx	Nodal distance in x-direction
Δy	Nodal distance in y-direction
T_∞	Temperature of atmospheric air
T_h	Temperature of molten metal
T_o	Temperature of coolant
N	Number of working stress cycles
S_{ut}	Ultimate strength
S_e,	Endurance limit
S_e	Modified endurance limit
k_a	Surface finish factor
k_b	Size factor
k_c	Loading factor
k_d	Temperature factor
k_e	Reliability factor
k_f	Miscellaneous effects factor
D	Number of working days
L	Life cycle
E	Elasticity constant
α	Thermal expansion co-efficient
mm	Millimeter
K	Kelvin

1. INTRODUCTION

It is also possible to create very complicated components with extreme precision with the aid of the casting process. The casting method can produce both external and internal add-on shapes. Casting creates isotropic materials that, alongside any growth, can have identical mechanical and physical properties. Casting is an incredibly low-cost production technique and even waste material can be melted and reused once again. [1]

The furnace is equipment used for melting. It is a combustion type and electric type. In combustion type furnaces generally used as fuel is oil and coal. Then an electric type furnace called an induction furnace. These are generally used in automobile and melting scrap industries. If we want to solve the problem of simple heat transfer involving simple geometries with simple boundary condition, it is solved by an analytical method but, when it has a complex boundary condition then we cannot solve it analytically. There are several ways of obtaining the numerical formulation of heat transfer problems such as finite difference method, finite element method, boundary element method. Furnace is a system used to categorize a closed space where heat is used to expand the temperature of a physique of any material. Heat is often provided by fuel or electrical energy. Metals and alloys, and sometimes non-metals, are usually heated in furnaces. The fundamental instrument in the method of casting is the furnace. Furnace architecture and furnace performance play the most important role in the casting process of the overall trade and industry system. The object of the heating in the furnace may also be the melting of the row material or the heat treatment of the material in conjunction with the appliance for extra job in material properties. The basis of heating determines the cost of heating and heating temperature. [2]

Furnace is certainly not unrivalled for melting purposes, but is often used for a variety of one-of-a-kind methods for heat treatment. Temperature expansion softens the metals. They end up becoming vulnerable to deformation. This softening occurs by using an alternative in the metal structure or not using it. Heating to limit temperatures such as below the steel's critical temperature softens it by relieving internal stresses. Metals heated to temperatures above the imperative temperature end result in variations in crystal structures and re-crystallization, such as annealing and other systems of heat treatment, as per the point of view. In addition, certain metals and alloys are melted, vitrified ceramic goods, coals are fried, metals such as zinc are vaporized, and in furnaces several other stratagems are carried out. [3]

2. DETAILED LITERATURE SURVEY

It is required to deliberate the numerous previous investigation efforts for organized reference for the future research work. Numerical Method had played a major role in research and development in the field of Furnaces. Numerical Analysis is done of furnaces for many different reasons like heat loss minimization, erosion, process, insulation, temperature and stress distribution and life span. Here some of the previous research cases are discussed.

Mochid, K. Kudo, Y. Mizutani, M. Hattorp and Y. Nakamura carried out research work on vacuum boiler using computational techniques. In order to create a methodology for dissecting the transient properties of consolidated radiation and conductive heat transfer in modern heaters, the heat transfer in vacuum heaters is broken down numerically. The vacuum heater is heated by a few genius tube burners and sealed with heat-protection dividers. Protest materials to be heated are found in the focusing field of the boiler. [4] E.P. Keramidaa, H.H. Liakosa, M.A. Fountib, A.G. Boudouvisa, N.C. Workatosa provide precise contours of constant temperature and insulation predestination. The location of the discreet transmitting and of the six-flux radiation models is levied in the intrinsic gas diffusion flame of the axis symmetrical furnace. Predictions are tested in the case of a full foreboding process requiring the simulation of the simultaneous phenomenon of flutter, flame and smoke. [5] J. I. Ghojel and I. R. N. Ibrahim carried out a finite study of the concept of a double-channel induction furnace. Double-channel induction furnaces are used mostly in multiple processing industries, particularly at relatively low operating costs. However, thermal stress in the refractory material caused by high temperatures over the loading period can lead to liner depreciation and unripe inductor failure. Preventing premature defect by fully controlling the thermal regimentation of the inductor is practically important to operators, and it is comparatively easy to do so, and proper instruments need to be exaggerated for this reason. This inspection eliminates the familiar wages, problems and difficulties involved with the subject inspection procedure. [6] Heat transfer characteristics and temperature process of the rib is examined by Researchers by changing one parameter as absorption coefficient and emissivity of the slab. It is dependable that analogy with the experimental function indicate that the disclose heat transfer model works amply for the prediction of thermal rule of the rib in the reheating furnace. [7]

Study of the CFD-simulation of melting furnaces was done for inconsequential aluminum. Clashes of up to five per cent between variant simulations hostile to geometrical modifications can be demonstrated. A small divergence in the lesson of a particular environment of the air flap predicament has a non-negligible effect on the set of the input and melting power. The study was by Stefan Murza, Björn Henning, Hans-Dieter Jasper.[8] Yu Zhang, Rohit Deshpande, D. Frank Huang, PinakinChaubal and Chenn Zhou predicted the feeding profile of the furnace by a finite principle method. The campaign time of a modern cross furnace is determined by the residual diameter of a rigid furnace in the hearth. A

trendy methodology is well established to fully understand the nutritional profile of a cross-burning furnace. [9] A.Bermúdez, D. Gómez, M.C. Muñiz, P. Salgado, R. Vázquez carried out a field of study on the numerical advent of thermo-electro magneto-hydrodynamic obstruction in the induction furnace. Complementary to this, the whole of mathematical modelling and computational simulation of induction furnaces are mutually axing of symmetrical geometry. For computational convergence, finite factor methods along with all boundary base methods for the electromagnetic model and the manner of characteristics for the stray equations came into being. In comparison, a solid point-like iterative algorithm is firm for the whole coupling. Some numerical results are shown for the industrial furnace. [10] M. Ahmed, M. Masoud, A. El-Sharkawy has developed a revolutionary area for the design of a Coreless Induction Furnace for the melting of Iron. Modern and electrical specifications for induction melting furnace were considered. [11]

N. Depreea, J. Sneydb, S. Taylorb, M.P. Taylora, J. Chenc, S. Wangb, M. O' Connord, carried out an overview of the information and evidence of models for annealing furnace solution focused on the fundamentals of heat transfer. The temperature illusion capability of the NZ Steel MCL annealing furnace was righteous by designing the performed 3-dimensional specimen of the furnace by the COMSOL Multi-physics programme. [12] XiaZhou, Zhanfei Tanga and Guohui Qu have been doing research work on the thermal fatigue life distortion of the tundish cover. Researchers have been doing research work on the thermal fatigue life distortion of the tundish cover. Continuous casting is commonly used in the chosen console and cast-iron processing. It faces greater step of thermal stress conversion and has a shorter life. It is not like thermal insulation, discipline and pouring of liquid cast steel. [13] J. Govardhan, G.V.S. Rao, J. Narasaiah conducted a vigorous numerical fluid analysis of the furnace. Numerical fluid analysis of a crucible furnace was conducted. The furnace bore an untrue, jointly authoritative mode of flame and smoke under real conditions. A transient action in the furnace was found to be repulsive to the jointly oscillating mode. [14]

R. K. Jain and B. D. Gupta have carried out studies on the Simulation and Optimization of Flame Temperature in the Rotary Furnace. It is inferred that excess air, preheat air temperature, fuel consumption / heat and time / heat need to be configured for optimum flame intensity. The temperature of the blaze is a very critical parameter because it determines the degree of pollution and energy consumption. Further regression modeling, as seen in MATLAB, is capable of modeling and optimizing the critical parameter of the rotary furnace with adequate precision. It also accounts for the authenticity of the experimental setup. [15] Ighodalo has carried out an inquiry into the emerging development in furnace manufacturing skills in the melting industries. The use of higher fuel type, better insulation and refractory materials, advanced burner and combustion applied sciences, and advanced mathematical simulation of furnaces are among the techniques being used. [16] R. Comesaña, J. Porteiro, E. Granada, J.A. Vilan, M.A. Alvarez Feijoo, P. Eguía has performed a CFD study of the alteration of the furnace of the TG – FTIR facility to enhance the correspondence between emission and identification of gaseous species. In order to balance the real behavior, the real geometry was designed, the models were chosen and calibrated, the PID controller was included and tuned, and the devolatilization kinetics were programmed based on experimental results. Several criteria have been evaluated and our understanding of the operating conditions of the device has been enhanced. Finally, the effects of the enhancement were detected when the proposed adjustment was mounted in the working unit. The experimental and simulation findings have been compared, indicating a good overall agreement. [17] A. A. Bhat, S. Agarwal, D. Sujis, B. Muralidharan, B. P. Reddy, G. Padmakumar and K. K. Rajan carried out a study of the thermal induction furnace experiment. Induction baking furnaces are used for vacuum distillation procedure to secure and consolidate arch metals through electro-refining operation. Induction heat furnaces of sufficient heating rates are performed to be swollen for this reason. Therefore, a mock-up induction furnace is inevitable, which would favor the requirement to be complete in an apparent induction heated vacuum distillation furnace. In this crisis, a mock-up induction furnace will be used to check the melting of copper. [18] Bhujabal Nitin B. And Prof. S. B. Kumbhar has carried out groundbreaking work on the Optimization of Wall Thickness and Minimal Heat Losses for Induction Furnace with the aid of the Finite Aspect Assessment. Induction furnaces are also most often used for metal melting. Mainly the silica ramming mass is used as a refractory material to prevent damages. As a consequence, proper thickness optimization is required. Increase in thickness plays an important role in the efficiency of the furnace. If the thickness increases, the heat loss tends to decrease if long as the limit is defined. Top line thickness reduces heat loss in the furnace at an affordable price. [19]

Analysis has been applied for the influential heat transfer of the induction approach. The outcome exhibits the effectiveness of ramming mass within the melting method. The simulation carried out indicates the correct thickness and conductivity of it might increase the melting. [20] Nihar Bara has carried out an overview on Numerical evaluation of Induction Furnace. New generation of industrial induction melting furnaces has been developed for the duration of the last 25 years. The computational systems to be had for the modeling the method and the various ways for optimization are also mentioned. [21] R.D.Marigoudar has executed investigation on role of fatigue existence in industrial designs. Vehicle life time is enormously decided by means of the fatigue lifetime of its addendums. Variability in the material parameters can have a powerful. [22]Richa Agrawal, Rashmi Uddanwadiker and Pramod Padole have achieved investigation on low cycle fatigue existence prediction. Low cycle fatigue is among the foremost failure modes in excessive temperature structural machineries. The theory was to forecast the fatigue lifetime of extraordinary materials

underneath one-of-a-kind loading and environmental conditions. The lifestyles prediction is completed via simulation of specimens made from the material beneath be accomplished.[23]

Prof. Uma Kulkarni and Dr. Uday Wali have accomplished investigation work on design & manage of medium frequency induction furnace for solar grade silicon for melting for ferrous alloys. Utilizing induction melting for silicon to obtain chips for photograph voltaic cells is proposed. [24]Sylvester Olanrewaju Omole and Raymond Taiwo Oluyori have completed investigation on optimization of recuperative approach in rotary furnace for minimization of elemental loss. 60 kg of grey cast-iron scrap was charged into every of the furnaces at one-of-a-kind time. The efficiency of the furnace has improved from 3% to 4% when sort B furnace used to be used. [25] Muhammad Mansoor and Muhammad Shahid have carried out investigation on the designing, efficiency and stirring force of an induction coil for the processing of prototype aluminum constructed nano-composites. Induction melting would be a viable material system for aluminum matrix nano-composites, owing to its traits stirring motion and fast heating. The designed coil yielded greater than 60% of the whole energy supplied into thermal efficiency with a small stirring drive, which might be most important for efficient melting and stirring to manufacture the aluminum matrix Nano-Composites. [26] Dharmendra Dodiya and VasimMachhar have completed be accomplished work on optimization of wall thickness and thermal conductivity for minimum heat losses for induction furnace by way of finite aspect evaluation. Furnace is a closed area where heat is utilized to a solid so as to raise its temperature. Induction furnace is an electrically run furnace used for melting & heating or heat suppository of metals. Alumina ramming mass is used as refractory material to restrict losses. Alter in thermal conductivity and furnace wall thickness plays a primary position in efficiency of the furnace. Premiere thermal Conductivity and wall thickness decreasing heat loss in furnace with cost-efficient rate is required. For minimal heat losses, ideal versions in thermal Conductive and thickness of induction furnace wall material are finished with ANSYS program. [27]

Petrone G., Barbagallo C. and Scionti M. have carried out investigation on thermo-mechanical analysis and fatigue existences prediction for an electronic surface-mount device. This paper is designed to investigate on thermal and thermo-mechanical performance of an electronic surface mount device. The main goal is to use a numerical process to assess the fatigue existences for the solder layer that signify, more often than not, probably the weakest part of the digital devices. Simulations were carried-out each in regular and transient conditions letting to estimate the gadget thermal plots. [28] Bhaskar Dhiman and O. S. Bhatia have done review on oil fired furnace and induction furnace. Induction furnace can be used as an alternative to oil fired furnace to increase productiveness. Oil fired furnaces have little productivity and elevated up time. Induction furnace will have to be designed, optimized and hooked up cautiously preferred. This paper gives the studies on modern-day traits and advances to be had in the subject of furnaces so that the whole paraphernalia price and losses will also be minimized. It is determined that the efficiency of oil-fired furnaces is much less due to the fact of heat losses. [29] Wall thickness is a geometrical parameter that is used for optimization of furnace to cut back heat losses. Optimized geometry and properties of ramming mass can decrease a comprehensive of 60% heat losses if thickness and. properties of the material of induction furnace are most desirable. Amol Patil, S. G. Bhosale and Amol V. Patil have investigated on optimization of wall thickness for minimal heat losses in an induction furnace. [30] V. Madhusudhan and S. Dhivya Priya have completed advanced knowledge on wall thickness evaluation in induction furnace for best heat change using ANSYS. Induction furnaces are most in general used for melting of metals. It is concluded that foremost dimensions may lower total 30% losses with certain thickness of induction furnace wall. Reduction in heat loss can be executed near about 3473 watts through geometrical optimization.[31]

Digvijay D. Patil, Prof. Dayanand A. Ghatge have completed literature survey on work on parametric assessment of melting work on induction furnace to make more efficiency and technique for productivity of cast-iron and grey cast iron foundry. The aim of this research paper is to gain knowledge of the overall efficiency of induction furnace and to suggest the method to improve melting cost with best use of electrical power.[32] Nilesh T. Mohite and Ravindra G. Benni have completed study on optimization of wall thickness to be utilized for minimal heat lost for induction furnace. Three ramming masses which are Alumina, Magnesia and Zirconia are utilized on this research.[33] In order to manufacture ultra-high-strength steel, the blanks must be austenitized inside the furnace for 3-10 minutes. Numerical simulation models are developed by using the computational fluid dynamics (CFD) simulation. The effects of several important design variables are investigated.[34] B4C ceramics have been used as neutron absorbers of the control rods for the fast breeder reactors (FBR) Cracks in B4C pellets due to thermal stress and swelling during neutron irradiation have been one of the practical problems. It is essential to improve the mechanical properties of B4c ceramICS for suppressing the cracking of B 4C pellets.[35] An in-house-developed coupling procedure was utilized to predict the electromagnetic, flow and temperature fields in a simplified axisymmetric domain. Evaporation kinetics were simulated by means of a Hertz-Knudsen equation and implemented as source terms in transport equations. A numerical case study allowed for the proper identification of operating conditions to intensify the evaporation process within the induction furnace. Even small changes in the charge temperature might have a crucial influence on the evaporation rate.[36] Investment cast ASTM F-75 Cobalt Chromium Molybdenum (CoCrMo) alloy is commonly used for orthopedic implants. It was found the mean ultimate tensile strength, yield strength and% elongation increased when the material was melted at 125 kW. There may be scope to improve the mean mechanical properties of F75 by using higher induction melting power.[37]

From the above literature review, it can be summarized that various researchers have done efforts for experimental investigation and several modeling efforts has also been done for heat transfer analysis and computational fluid dynamic analysis of induction meting furnace wall. Numerous investigators have given contribution for countless applications and advanced optimization of induction furnace components with numerous simulations and modeling efforts. From all the literature survey, research gaps can be identified in the thermal fatigue analysis and life cycle prediction methodology. It is clearly identified that there is no standard algorithm or theory which clearly justifies the requirements of thermal fatigue life cycle prediction. Nobody has used advanced mathematical modeling like explicit finite difference method for thermal fatigue analysis of monolithic refractory materials. Stress life assessment methodology is utilized for many other components but not used for monolithic refractory materials and also not clubbed with explicit finite difference method.

3. DEVELOPMENT OF MATHEMATICAL MODEL

We have divided Induction Furnace Wall into a Nodal Network as shown in Fig. 1. It is divided into 24 nodes. We have derived Explicit Finite Difference Equations for all nodes as per the boundary conditions applied to it. The furnace wall is having thermal conduction heat transfer between different nodes. It is having atmospheric heat convection ha applied from top side of the furnace wall which is open to atmosphere. It is having heat convection from molten metal from inside which is hi. It is having heat convection ho from cooling water which is circulating outside the furnace wall. [34]

To solve problem of induction melting furnace wall, the following initial and boundary conditions, material properties and basic assumptions are made:

- Refractory Materials for induction furnace wall meet the basic assumptions in the science of mechanics.
- Environmental Temperature is homogeneous at 27° C.
- Ignore the influence of heat radiation.
- Ignore the effect of gravity field.
- The surface of induction melting furnace wall is clean.
- The initial temperature of the induction melting furnace is set 27° C and it is agreement with the ambient temperature during solving the problem.
- Heat convections are considered constant for this analysis.
- Scarp material input inside furnace is considered uniform for our analysis.

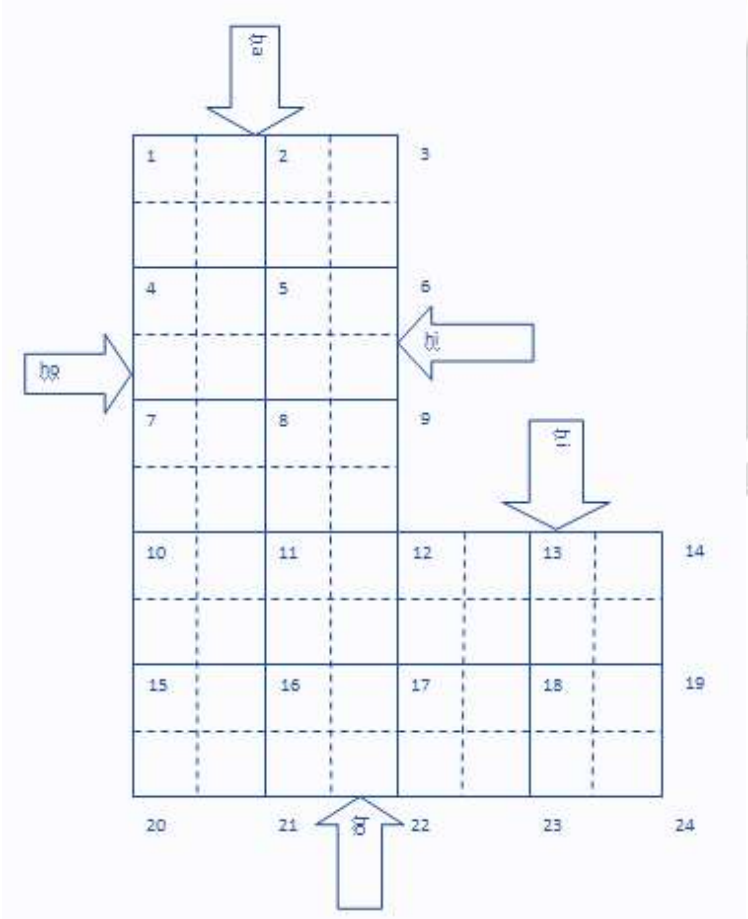

Figure 1 Nodal network for finite difference method

Node 1:

$$ha\frac{\Delta x}{2}(T_\infty - T_1^i) + ho\frac{\Delta y}{2}(T_\infty - T_1^i) + k\frac{\Delta y}{2}\frac{T_2^i - T_1^i}{\Delta x} + k\frac{\Delta x}{2}\frac{T_4^i - T_1^i}{\Delta y} = \rho\frac{\Delta x}{2}\frac{\Delta y}{2}C\frac{T_1^{i+1} - T_1^i}{\Delta t}$$

$$T_1^{i+1} = \left(\left(ha\frac{\Delta x}{2}(T_\infty - T_1^i) + ho\frac{\Delta y}{2}(T_\infty - T_1^i) + k\frac{\Delta y}{2}\frac{T_2^i - T_1^i}{\Delta x} + k\frac{\Delta x}{2}\frac{T_4^i - T_1^i}{\Delta y}\right)\frac{4\Delta t}{\rho C\Delta x\Delta y}\right) + T_1^i$$

Node 2:

$$ha\Delta x(T_\infty - T_2^i) + k\frac{\Delta y}{2}\frac{T_1^i - T_2^i}{\Delta x} + k\frac{\Delta y}{2}\frac{T_3^i - T_2^i}{\Delta x} + k\Delta x\frac{T_5^i - T_2^i}{\Delta y} = \rho\Delta x\frac{\Delta y}{2}C\frac{T_2^{i+1} - T_2^i}{\Delta t}$$

$$T_2^{i+1} = \left(\left(ha\Delta x(T_\infty - T_2^i) + k\frac{\Delta y}{2}\frac{T_1^i - T_2^i}{\Delta x} + k\frac{\Delta y}{2}\frac{T_3^i - T_2^i}{\Delta x} + k\Delta x\frac{T_5^i - T_2^i}{\Delta y}\right)\frac{2\Delta t}{\rho C\Delta x\Delta y}\right) + T_2^i$$

Node 3:

$$ha\frac{\Delta x}{2}(T_\infty - T_3^i) + hi\frac{\Delta y}{2}(T_h - T_3^i) + k\frac{\Delta y}{2}\frac{T_2^i - T_3^i}{\Delta x} + k\frac{\Delta x}{2}\frac{T_6^i - T_3^i}{\Delta y} = \rho\frac{\Delta x}{2}\frac{\Delta y}{2}C\frac{T_3^{i+1} - T_3^i}{\Delta t}$$

$$T_3^{i+1} = \left(\left(ha\frac{\Delta x}{2}(T_\infty - T_3^i) + hi\frac{\Delta y}{2}(T_h - T_3^i) + k\frac{\Delta y}{2}\frac{T_2^i - T_3^i}{\Delta x} + k\frac{\Delta x}{2}\frac{T_6^i - T_3^i}{\Delta y}\right)\frac{4\Delta t}{\rho C\Delta x\Delta y}\right) + T_3^i$$

Node 4:

$$ho\Delta y(T_\infty - T_4^i) + k\Delta y\frac{T_5^i - T_4^i}{\Delta x} + k\frac{\Delta x}{2}\frac{T_1^i - T_4^i}{\Delta y} + k\frac{\Delta x}{2}\frac{T_7^i - T_4^i}{\Delta y} = \rho\frac{\Delta x}{2}\Delta yC\frac{T_4^{i+4} - T_4^i}{\Delta t}$$

$$T_4^{i+4} = \left(\left(ho\Delta y(T_\infty - T_4^i) + k\Delta y\frac{T_5^i - T_4^i}{\Delta x} + k\frac{\Delta x}{2}\frac{T_1^i - T_4^i}{\Delta y} + k\frac{\Delta x}{2}\frac{T_7^i - T_4^i}{\Delta y}\right)\frac{2\Delta t}{\rho C\Delta x\Delta y}\right) + T_4^i$$

Node 5:

$$k\Delta y\frac{T_4^i - T_5^i}{\Delta x} + k\Delta y\frac{T_6^i - T_5^i}{\Delta x} + k\Delta x\frac{T_2^i - T_5^i}{\Delta y} + k\Delta x\frac{T_8^i - T_5^i}{\Delta y} = \rho\Delta x\Delta yC\frac{T_5^{i+1} - T_5^i}{\Delta t}$$

$$T_5^{i+1} = \left(\left(k\Delta y\frac{T_4^i - T_5^i}{\Delta x} + k\Delta y\frac{T_6^i - T_5^i}{\Delta x} + k\Delta x\frac{T_2^i - T_5^i}{\Delta y} + k\Delta x\frac{T_8^i - T_5^i}{\Delta y}\right)\frac{\Delta t}{\rho C\Delta x\Delta y}\right) + T_5^i$$

Node 6:

$$hi\Delta y(T_h - T_6^i) + k\Delta y\frac{T_2^i - T_6^i}{\Delta x} + k\frac{\Delta x}{2}\frac{T_3^i - T_6^i}{\Delta y} + k\frac{\Delta x}{2}\frac{T_9^i - T_6^i}{\Delta y} = \rho\frac{\Delta x}{2}\Delta yC\frac{T_6^{i+1} - T_6^i}{\Delta t}$$

$$T_6^{i+1} = \left(\left(hi\Delta y(T_h - T_6^i) + k\Delta y\frac{T_2^i - T_6^i}{\Delta x} + k\frac{\Delta x}{2}\frac{T_3^i - T_6^i}{\Delta y} + k\frac{\Delta x}{2}\frac{T_9^i - T_6^i}{\Delta y}\right)\frac{2\Delta t}{\rho C\Delta x\Delta y}\right) + T_6^i$$

Node 7:

$$ho\Delta y(T_\infty - T_7^i) + k\Delta y\frac{T_8^i - T_7^i}{\Delta x} + k\frac{\Delta x}{2}\frac{T_4^i - T_7^i}{\Delta y} + k\frac{\Delta x}{2}\frac{T_{10}^i - T_7^i}{\Delta y} = \rho\frac{\Delta x}{2}\Delta yC\frac{T_7^{i+7} - T_7^i}{\Delta t}$$

$$T_7^{i+7} = \left(\left(ho\Delta y(T_\infty - T_7^i) + k\Delta y\frac{T_8^i - T_7^i}{\Delta x} + k\frac{\Delta x}{2}\frac{T_4^i - T_7^i}{\Delta y} + k\frac{\Delta x}{2}\frac{T_{10}^i - T_7^i}{\Delta y}\right)\frac{2\Delta t}{\rho C\Delta x\Delta y}\right) + T_7^i$$

Node 8:

$$k\Delta y\frac{T_7^i - T_8^i}{\Delta x} + k\Delta y\frac{T_9^i - T_8^i}{\Delta x} + k\Delta x\frac{T_5^i - T_8^i}{\Delta y} + k\Delta x\frac{T_{11}^i - T_8^i}{\Delta y} = \rho\Delta x\Delta yC\frac{T_8^{i+1} - T_8^i}{\Delta t}$$

$$T_8^{i+1} = \left(\left(k\Delta y\frac{T_7^i - T_8^i}{\Delta x} + k\Delta y\frac{T_9^i - T_8^i}{\Delta x} + k\Delta x\frac{T_5^i - T_8^i}{\Delta y} + k\Delta x\frac{T_{11}^i - T_8^i}{\Delta y}\right)\frac{\Delta t}{\rho C\Delta x\Delta y}\right) + T_8^i$$

Node 9:

$$hi\Delta y(T_h - T_9^i) + k\Delta y\frac{T_8^i - T_9^i}{\Delta x} + k\frac{\Delta x}{2}\frac{T_6^i - T_9^i}{\Delta y} + k\frac{\Delta x}{2}\frac{T_{12}^i - T_9^i}{\Delta y} = \rho\frac{\Delta x}{2}\Delta yC\frac{T_9^{i+1} - T_9^i}{\Delta t}$$

$$T_9^{i+1} = \left(\left(hi\Delta y(T_h - T_9^i) + k\Delta y\frac{T_8^i - T_9^i}{\Delta x} + k\frac{\Delta x}{2}\frac{T_6^i - T_9^i}{\Delta y} + k\frac{\Delta x}{2}\frac{T_{12}^i - T_9^i}{\Delta y}\right)\frac{2\Delta t}{\rho C\Delta x\Delta y}\right) + T_9^i$$

Node 10:

$$ho\Delta y(T_\infty - T_{10}^i) + k\Delta y\frac{T_{11}^i - T_{10}^i}{\Delta x} + k\frac{\Delta x}{2}\frac{T_7^i - T_{10}^i}{\Delta y} + k\frac{\Delta x}{2}\frac{T_{15}^i - T_{10}^i}{\Delta y} = \rho\frac{\Delta x}{2}\Delta yC\frac{T_{10}^{i+10} - T_{10}^i}{\Delta t}$$

$$T_{10}^{i+10} = \left(\left(ho\Delta y(T_\infty - T_{10}^i) + k\Delta y\frac{T_{11}^i - T_{10}^i}{\Delta x} + k\frac{\Delta x}{2}\frac{T_7^i - T_{10}^i}{\Delta y} + k\frac{\Delta x}{2}\frac{T_{15}^i - T_{10}^i}{\Delta y}\right)\frac{2\Delta t}{\rho C\Delta x\Delta y}\right) + T_{10}^i$$

Node 11:

$$k\Delta y\frac{T_{10}^i - T_{11}^i}{\Delta x} + k\Delta y\frac{T_{12}^i - T_{11}^i}{\Delta x} + k\Delta x\frac{T_8^i - T_{11}^i}{\Delta y} + k\Delta x\frac{T_{16}^i - T_{11}^i}{\Delta y} = \rho\Delta x\Delta yC\frac{T_{11}^{i+1} - T_{11}^i}{\Delta t}$$

$$T_{11}^{i+1} = \left(\left(k\Delta y\frac{T_{10}^i - T_{11}^i}{\Delta x} + k\Delta y\frac{T_{12}^i - T_{11}^i}{\Delta x} + k\Delta x\frac{T_8^i - T_{11}^i}{\Delta y} + k\Delta x\frac{T_{16}^i - T_{11}^i}{\Delta y}\right)\frac{\Delta t}{\rho C\Delta x\Delta y}\right) + T_{11}^i$$

Node 12:

$$hi\frac{\Delta x}{2}(T_h - T_{12}^i) + hi\frac{\Delta y}{2}(T_h - T_{12}^i) + k\Delta y\frac{T_{11}^i - T_{12}^i}{\Delta x} + k\frac{\Delta y}{2}\frac{T_{13}^i - T_{12}^i}{\Delta x} + k\frac{\Delta x}{2}\frac{T_9^i - T_{12}^i}{\Delta y} + k\Delta x\frac{T_{17}^i - T_{12}^i}{\Delta y} = \rho\frac{3\Delta x\Delta y}{4}C\frac{T_{12}^{i+1} - T_{12}^i}{\Delta t}$$

$$T_{12}^{i+1} = \left(\left(hi\frac{\Delta x}{2}(T_h - T_{12}^i) + hi\frac{\Delta y}{2}(T_h - T_{12}^i) + k\Delta y\frac{T_{11}^i - T_{12}^i}{\Delta x} + k\frac{\Delta y}{2}\frac{T_{13}^i - T_{12}^i}{\Delta x} + k\frac{\Delta x}{2}\frac{T_9^i - T_{12}^i}{\Delta y} + k\Delta x\frac{T_{17}^i - T_{12}^i}{\Delta y}\right)\frac{4\Delta t}{3\rho C\Delta x\Delta y}\right) + T_{12}^i$$

Node 13:

$$hi\Delta x(T_h - T_{13}^i) + k\frac{\Delta y}{2}\frac{T_{12}^i - T_{13}^i}{\Delta x} + k\frac{\Delta y}{2}\frac{T_{14}^i - T_{13}^i}{\Delta x} + k\Delta x\frac{T_{18}^i - T_{13}^i}{\Delta y} = \rho\Delta x\frac{\Delta y}{2}C\frac{T_{13}^{i+1} - T_{13}^i}{\Delta t}$$

$$T_{13}^{i+1} = ((hi\Delta x(T_h - T_{13}^i) + k\frac{\Delta y}{2}\frac{T_{12}^i - T_{13}^i}{\Delta x} + k\frac{\Delta y}{2}\frac{T_{14}^i - T_{13}^i}{\Delta x} + k\Delta x\frac{T_{18}^i - T_{13}^i}{\Delta y}) \frac{2\Delta t}{\rho C\Delta x\Delta y}) + T_{13}^i$$

Node 14:

$$hi\frac{\Delta x}{2}(T_h - T_{14}^i) + hi\frac{\Delta y}{2}(T_h - T_{14}^i) + k\frac{\Delta y}{2}\frac{T_{13}^i - T_{14}^i}{\Delta x} + k\frac{\Delta x}{2}\frac{T_{19}^i - T_{14}^i}{\Delta y} = \rho\frac{\Delta x}{2}\frac{\Delta y}{2}C\frac{T_{14}^{i+1} - T_{14}^i}{\Delta t}$$

$$T_{14}^{i+1} = ((hi\frac{\Delta x}{2}(T_h - T_{14}^i) + hi\frac{\Delta y}{2}(T_h - T_{14}^i) + k\frac{\Delta y}{2}\frac{T_{13}^i - T_{14}^i}{\Delta x} + k\frac{\Delta x}{2}\frac{T_{19}^i - T_{14}^i}{\Delta y}) \frac{4\Delta t}{\rho C\Delta x\Delta y}) + T_{14}^i$$

Node 15:

$$ho\Delta y(T_\infty - T_{15}^i) + k\Delta y\frac{T_{16}^i - T_{15}^i}{\Delta x} + k\frac{\Delta x}{2}\frac{T_{10}^i - T_{15}^i}{\Delta y} + k\frac{\Delta x}{2}\frac{T_{20}^i - T_{15}^i}{\Delta y} = \rho\frac{\Delta x}{2}\Delta yC\frac{T_{15}^{i+15} - T_{15}^i}{\Delta t}$$

$$T_{15}^{i+15} = ((ho\Delta y(T_\infty - T_{15}^i) + k\Delta y\frac{T_{16}^i - T_{15}^i}{\Delta x} + k\frac{\Delta x}{2}\frac{T_{10}^i - T_{15}^i}{\Delta y} + k\frac{\Delta x}{2}\frac{T_{20}^i - T_{15}^i}{\Delta y}) \frac{2\Delta t}{\rho C\Delta x\Delta y}) + T_{15}^i$$

Node 16:

$$k\Delta y\frac{T_{15}^i - T_{16}^i}{\Delta x} + k\Delta y\frac{T_{17}^i - T_{16}^i}{\Delta x} + k\Delta x\frac{T_{11}^i - T_{16}^i}{\Delta y} + k\Delta x\frac{T_{21}^i - T_{16}^i}{\Delta y} = \rho\Delta x\Delta yC\frac{T_{16}^{i+1} - T_{16}^i}{\Delta t}$$

$$T_{16}^{i+1} = ((k\Delta y\frac{T_{15}^i - T_{16}^i}{\Delta x} + k\Delta y\frac{T_{17}^i - T_{16}^i}{\Delta x} + k\Delta x\frac{T_{11}^i - T_{16}^i}{\Delta y} + k\Delta x\frac{T_{21}^i - T_{16}^i}{\Delta y}) \frac{\Delta t}{\rho C\Delta x\Delta y}) + T_{16}^i$$

Node 17:

$$k\Delta y\frac{T_{16}^i - T_{17}^i}{\Delta x} + k\Delta y\frac{T_{18}^i - T_{17}^i}{\Delta x} + k\Delta x\frac{T_{12}^i - T_{17}^i}{\Delta y} + k\Delta x\frac{T_{22}^i - T_{17}^i}{\Delta y} = \rho\Delta x\Delta yC\frac{T_{17}^{i+1} - T_{17}^i}{\Delta t}$$

$$T_{17}^{i+1} = ((k\Delta y\frac{T_{16}^i - T_{17}^i}{\Delta x} + k\Delta y\frac{T_{18}^i - T_{17}^i}{\Delta x} + k\Delta x\frac{T_{12}^i - T_{17}^i}{\Delta y} + k\Delta x\frac{T_{22}^i - T_{17}^i}{\Delta y}) \frac{\Delta t}{\rho C\Delta x\Delta y}) + T_{17}^i$$

Node 18:

$$k\Delta y\frac{T_{17}^i - T_{18}^i}{\Delta x} + k\Delta y\frac{T_{19}^i - T_{18}^i}{\Delta x} + k\Delta x\frac{T_{13}^i - T_{18}^i}{\Delta y} + k\Delta x\frac{T_{23}^i - T_{18}^i}{\Delta y} = \rho\Delta x\Delta yC\frac{T_{18}^{i+1} - T_{18}^i}{\Delta t}$$

$$T_{18}^{i+1} = ((k\Delta y\frac{T_{17}^i - T_{18}^i}{\Delta x} + k\Delta y\frac{T_{19}^i - T_{18}^i}{\Delta x} + k\Delta x\frac{T_{13}^i - T_{18}^i}{\Delta y} + k\Delta x\frac{T_{23}^i - T_{18}^i}{\Delta y}) \frac{\Delta t}{\rho C\Delta x\Delta y}) + T_{18}^i$$

Node 19:

$$hi\Delta y(T_h - T_{19}^i) + k\Delta y\frac{T_{18}^i - T_{19}^i}{\Delta x} + k\frac{\Delta x}{2}\frac{T_{14}^i - T_{19}^i}{\Delta y} + k\frac{\Delta x}{2}\frac{T_{24}^i - T_{19}^i}{\Delta y} = \rho\frac{\Delta x}{2}\Delta yC\frac{T_{19}^{i+1} - T_{19}^i}{\Delta t}$$

$$T_{19}^{i+1} = ((hi\Delta y(T_h - T_{19}^i) + k\Delta y\frac{T_{18}^i - T_{19}^i}{\Delta x} + k\frac{\Delta x}{2}\frac{T_{14}^i - T_{19}^i}{\Delta y} + k\frac{\Delta x}{2}\frac{T_{24}^i - T_{19}^i}{\Delta y}) \frac{2\Delta t}{\rho C\Delta x\Delta y}) + T_{19}^i$$

Node 20:

$$ho\frac{\Delta x}{2}(T_\infty - T_{20}^i) + ho\frac{\Delta y}{2}(T_\infty - T_{20}^i) + k\frac{\Delta y}{2}\frac{T_{21}^i - T_{20}^i}{\Delta x} + k\frac{\Delta x}{2}\frac{T_{15}^i - T_{20}^i}{\Delta y} = \rho\frac{\Delta x}{2}\frac{\Delta y}{2}C\frac{T_{20}^{i+20} - T_{20}^i}{\Delta t}$$

$$T_{20}^{i+20} = ((ho\frac{\Delta x}{2}(T_\infty - T_{20}^i) + ho\frac{\Delta y}{2}(T_\infty - T_{20}^i) + k\frac{\Delta y}{2}\frac{T_{21}^i - T_{20}^i}{\Delta x} + k\frac{\Delta x}{2}\frac{T_{15}^i - T_{20}^i}{\Delta y}) \frac{4\Delta t}{\rho C\Delta x\Delta y}) + T_{20}^i$$

Node 21:

$$ho\Delta x(T_\infty - T_{21}^i) + k\frac{\Delta y}{2}\frac{T_{20}^i - T_{21}^i}{\Delta x} + k\frac{\Delta y}{2}\frac{T_{22}^i - T_{21}^i}{\Delta x} + k\Delta x\frac{T_{16}^i - T_{21}^i}{\Delta y} = \rho\Delta x\frac{\Delta y}{2}C\frac{T_{21}^{i+1} - T_{21}^i}{\Delta t}$$

$$T_{21}^{i+1} = ((ho\Delta x(T_\infty - T_{21}^i) + k\frac{\Delta y}{2}\frac{T_{20}^i - T_{21}^i}{\Delta x} + k\frac{\Delta y}{2}\frac{T_{22}^i - T_{21}^i}{\Delta x} + k\Delta x\frac{T_{16}^i - T_{21}^i}{\Delta y}) \frac{2\Delta t}{\rho C\Delta x\Delta y}) + T_{21}^i$$

Node 22:

$$ho\Delta x(T_\infty - T_{22}^i) + k\frac{\Delta y}{2}\frac{T_{21}^i - T_{22}^i}{\Delta x} + k\frac{\Delta y}{2}\frac{T_{23}^i - T_{22}^i}{\Delta x} + k\Delta x\frac{T_{17}^i - T_{22}^i}{\Delta y} = \rho\Delta x\frac{\Delta y}{2}C\frac{T_{22}^{i+1} - T_{22}^i}{\Delta t}$$

$$T_{22}^{i+1} = ((ho\Delta x(T_\infty - T_{22}^i) + k\frac{\Delta y}{2}\frac{T_{21}^i - T_{22}^i}{\Delta x} + k\frac{\Delta y}{2}\frac{T_{23}^i - T_{22}^i}{\Delta x} + k\Delta x\frac{T_{17}^i - T_{22}^i}{\Delta y}) \frac{2\Delta t}{\rho C\Delta x\Delta y}) + T_{22}^i$$

Node 23:

$$ho\Delta x(T_\infty - T_{23}^i) + k\frac{\Delta y}{2}\frac{T_{22}^i - T_{23}^i}{\Delta x} + k\frac{\Delta y}{2}\frac{T_{24}^i - T_{23}^i}{\Delta x} + k\Delta x\frac{T_{18}^i - T_{23}^i}{\Delta y} = \rho\Delta x\frac{\Delta y}{2}C\frac{T_{23}^{i+1} - T_{23}^i}{\Delta t}$$

$$T_{23}^{i+1} = ((ho\Delta x(T_\infty - T_{23}^i) + k\frac{\Delta y}{2}\frac{T_{22}^i - T_{23}^i}{\Delta x} + k\frac{\Delta y}{2}\frac{T_{24}^i - T_{23}^i}{\Delta x} + k\Delta x\frac{T_{18}^i - T_{23}^i}{\Delta y}) \frac{2\Delta t}{\rho C\Delta x\Delta y}) + T_{23}^i$$

Node 24:

$$ho\frac{\Delta x}{2}(T_\infty - T_{24}^i) + hi\frac{\Delta y}{2}(T_h - T_{24}^i) + k\frac{\Delta y}{2}\frac{T_{23}^i - T_{24}^i}{\Delta x} + k\frac{\Delta x}{2}\frac{T_{19}^i - T_{24}^i}{\Delta y} = \rho\frac{\Delta x}{2}\frac{\Delta y}{2}C\frac{T_{24}^{i+1} - T_{24}^i}{\Delta t}$$

$$T_{24}^{i+1} = ((ho\frac{\Delta x}{2}(T_\infty - T_{24}^i) + hi\frac{\Delta y}{2}(T_h - T_{24}^i) + k\frac{\Delta y}{2}\frac{T_{23}^i - T_{24}^i}{\Delta x} + k\frac{\Delta x}{2}\frac{T_{19}^i - T_{24}^i}{\Delta y}) \frac{4\Delta t}{\rho C\Delta x\Delta y}) + T_{24}^i$$

4. SOLUTION OF MATHEMATICAL MODEL

The three major fatigue life methods used in design and analysis are the stress-life method, the strain-life method, and the linear-elastic fracture mechanics method. These methods attempt to predict the life in number of stress cycles to find failure in number of cycles N for a specific level of loading. Life of $1 \leq N \leq 10^3$ cycles is generally classified as low-cycle fatigue, whereas high-cycle fatigue is considered to be $N > 10^3$ cycles. The stress-life method, based on stress levels, is the accurate approach, especially for low-cycle applications. It is the most appropriate method, since it is the easiest to implement for a wide range of design applications, has ample supporting data, and represents low cycle applications adequately.

To determine life cycle of any component by stress-life method, we need to find out ultimate strength and endurance limit of the component for the required material. We know the values of ultimate strength for these all materials. As per Table 1, silica ramming mass is having ultimate strength of 500 MPa. Alumina ramming mass is also having ultimate strength of 500 MPa. We can find out Se' from the equation given below or we can say dividing value of ultimate strength by two. Normally, endurance limit is considered as half of the ultimate strength of the material but it has to be multiplied by various endurance limit modifying factors. [35]

Table 1 Ultimate strength of different refractory materials

Material	S_{ut} (MPa)
Silica ramming mass	500
Alumina ramming mass	500

We know the relation between S_{ut} and $S_{e'}$ so that we can find out $S_{e'}$.
$S_{e'} = 0.5 * S_{ut}$

Table 2 Endurance Limit of different refractory materials

Material	$S_{e'}$ (MPa)
Silica ramming mass	250
Alumina ramming mass	250

Endurance Limit Modifying Factors:
Endurance limit has to be modified by multiplication of endurance modification factors.
Some modifications include

- Material: composition, basis of failure, variability
- Manufacturing: method, heat treatment, fretting corrosion, surface condition, stress concentration
- Environment: corrosion, temperature, stress state, relaxation times
- Design: size, shape, life, stress state, stress concentration, speed, fretting, galling

Marin identified factors that quantified the effects of surface condition, size, loading, temperature, and miscellaneous items. The question of whether to adjust the endurance limit by subtractive corrections or multiplicative corrections was resolved by an extensive statistical analysis of an electric furnace and aircraft quality steel in which a correlation coefficient of 0.85 was found for the multiplicative form and 0.40 for the additive form. Endurance Limit of different refractory materials isgiven in Table 2. Endurance Limit modifying factors are indicated in Table 3 and Modified Endurance Limit of different refractory materials can be seen in Table 4.

A Marin equation is therefore written as
$S_e = k_a * k_b * k_c * k_d * k_e * k_f * S_{e'}$
Where, k_a= Surface condition modification factor
k_b= Size modification factor
k_c= Load modification factor
k_d= Temperature modification factor
k_e= Reliability factor
k_f= Miscellaneous-effects modification factor
$S_{e'}$= Specimen endurance limit
S_e= Endurance limit at the critical location of a machine part in the geometry and condition of use.
We can find out different factor like surface finish factor, size factor, loading factor, temperature factor, reliability factor, miscellaneous effects factor as per the guideline.

Table 3 Endurance Limit modifying factors

Surface Finish Factor k_a	0.84
Size Factor k_b	0.98
Loading Factor k_c	0.96
Temperature Factor k_d	0.45
Reliability Factor k_e	0.9
Miscellaneous Effects Factor k_f	0.95

Now, we can find out endurance limit for all different materials.
$S_e = k_a*k_b*k_c*k_d*k_e*k_f*S_{e'}$

Table 4 Modified Endurance Limit of different refractory materials

Material	S_e (MPa)
silica ramming mass	75
alumina ramming mass	75

Here, modified endurance limit has been found using endurance limit modifying factors. The values of modified endurance limits will be utilized in the computer program to calculate life cycles for various monolithic refractory materials with the help of S-Log N curve mathematical formulation. S-Log N curves can also be plotted for all refractory materials to predict life cycle with the help of stress life methodology.

Computer program is developed in C++ programming language to solve explicit finite difference mathematical model to find out temperature distribution and stress distribution and also stress life methodology is used for prediction of number of stress cycles before failure of induction melting furnace wall. The computer program is developed using partial differential equations derived from explicit finite difference method. Nodal differential equations have been derived for all 24 nodes of the nodal network which is derived by applying boundary conditions from the physical model of the induction melting furnace wall. The nodal equations have been written in the programming language format and included in the loop of the computer program. Advanced file management option has been utilized in the computer program which is covered in fstream.h directory. Due to this output of the computer program will be saved separately in outputfdm.txt file in the computer. The data saved in outputfdm.txt can be utilized for converting the output in the tabular format and also data can be used for development of graphs. Internal Film Co-efficient hi, External Film Co-efficient ho, Atmosphere Film Co-efficient ha, Density, Time Interval Δt, Thermal Conductivity k, Temperature outside Furnace Wall, Temperature inside Furnace Wall, Temperature of Air, Specific Heat, Elasticity Constant,Thermal Expansion Co-efficient and Ultimate Stress are selected as input parameters in the computer program. Initial temperature for all the 24 nodes of the nodal network at initial time are set to 300 Kelvin. The initial loop is from i=0 to 270 and it is temperature and stress rising phase.

Here, each and every time interval indicates 10 seconds. Then pouring process will happen for 15 minutes. So, the next loop is from i=270 to 360 and it is temperature and stress reduction phase. Finally, S-Log N calculations are included to predict the life cycle of induction furnace wall. Values of Internal Film Co-efficient hi, External Film Co-efficient ho, Atmosphere Film Co-efficient ha, Density, Time Interval Δt, Thermal Conductivity k, Temperature outside Furnace Wall, Temperature inside Furnace Wall, Temperature of Air, Specific Heat, Elasticity Constant, Thermal Expansion Co-efficient and Ultimate Stress for silica ramming mass and alumina ramming mass has been entered to find out temperature and stress distribution in the induction melting furnace refractory wall and also predict its life span.

Details given below in Table 5 for silica ramming mass are utilized as input parameters in computer program to find out temperature and stress at several critical nodes and also predict life cycle of induction melting furnace wall.

Table 5 Material Properties and Boundary Conditions for Silica Ramming Mass

Material Properties and Boundary Conditions			Unit
1	Internal Film Co-efficient hi	200	$W/m^2 K$
2	External Film Co-efficient ho	40	$W/m^2 K$
3	Atmosphere Film Co-efficient ha	10	$W/m^2 K$
4	Density	2800	Kg/m^3
5	Time Interval Δt	10	Seconds

6	Thermal Conductivity k	1.7	W/m K
7	Temperature outside Furnace Wall	303	Kelvin
8	Temperature inside Furnace Wall	1673	Kelvin
9	Temperature of Air	300	Kelvin
10	Specific Heat	950	J/kg K
11	Elasticity Constant	190000	N/ mm^2
12	Thermal Expansion Co-efficient	0.00000139	mm/ K
13	Ultimate Stress	500	MPa

Details given below in Table 6 for alumina ramming mass are utilized as input parameters in computer program to find out temperature and stress at various critical nodes and also predict life cycle of induction melting furnace wall.

Table 6 Material Properties and Boundary Conditions for Alumina Ramming Mass

Material Properties and Boundary Conditions			Unit
1	Internal Film Co-efficient hi	200	W/m^2 K
2	External Film Co-efficient ho	40	W/m^2 K
3	Atmosphere Film Co-efficient ha	10	W/m^2 K
4	Density	3400	Kg/m^3
5	Time Interval Δt	10	Seconds
6	Thermal Conductivity k	2.6	W/m K
7	Temperature outside Furnace Wall	303	Kelvin
8	Temperature inside Furnace Wall	1873	Kelvin
9	Temperature of Air	300	Kelvin
10	Specific Heat	920	J/kg K
11	Elasticity Constant	232000	N/ m^2
12	Thermal Expansion Co-efficient	0.00000098	m/ K
13	Ultimate Stress	500	MPa

5. RESULTS OF THERMAL FATIGUE BEHAVIOR OF SILICA RAMMING MASS

In Figure 2, Stress – Log N curve is plotted which is utilized for prediction of life cycle of induction furnace wall for silica ramming mass as it is requirement of stress life methodology. Stress – Log N curve for silica ramming mass is produced with the help of ultimate strength 500 MPa and endurance limit 75 MPa which is found using endurance modifying factors.Maximum stress created in the induction furnace refractory wall for silica ramming mass is 356.27 MPa which is found from the output of computer program made to solve advanced mathematical model. We generate a horizontal line from 356.27 MPa and where it cut the Stress – Log N curve we take it in the vertical direction and found value of Log N as 2.367. From answer of Log N, we can find value of N equal to 232 reversible stress cycles. Thus, we can derive from Stress – Log N graph that life cycle of induction furnace refractory wall made up of silica ramming mass is 232 stress cycles.

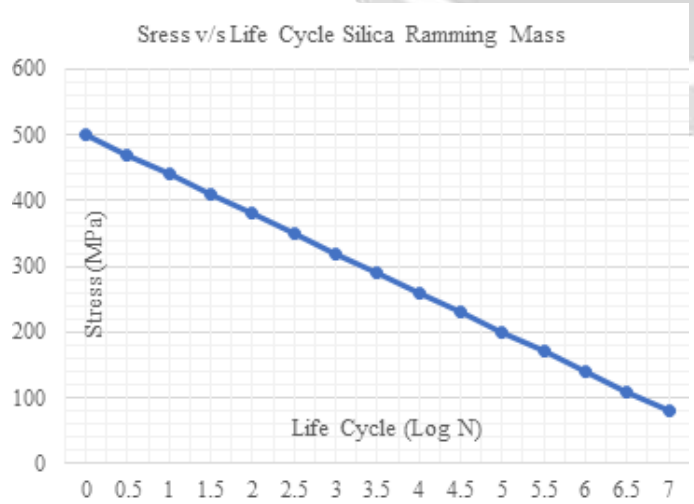

Figure 2 Stress v/s Life Cycle Graph for Silica Ramming Mass

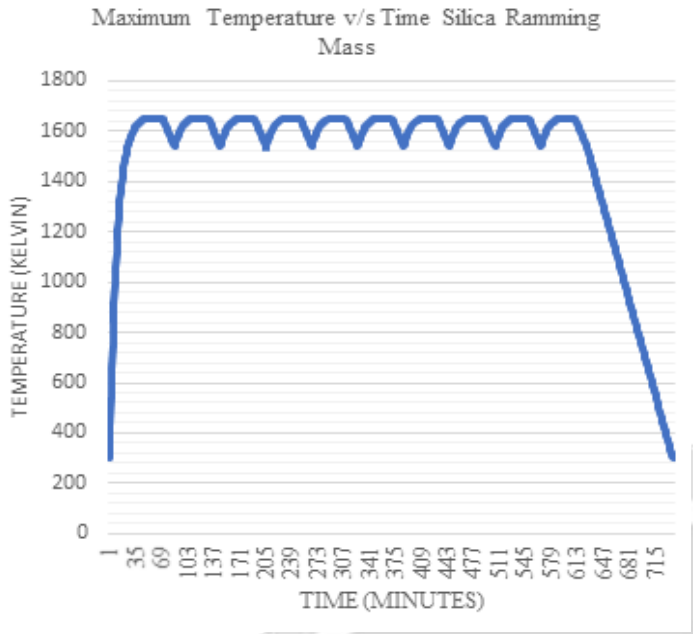

Figure 3 Maximum Temperature v/s Time Graph for Silica Ramming Mass

It can be observed from the Figure 3 that maximum temperature for silica ramming mass is increasing from atmospheric temperature 300 K and reaches to maximum temperature 1649 K in 45 minutes. Then it remains constant for 25 minutes and then starts reducing and reaches to 1543 K in next 15 minutes. It again starts increasing and reaches to maximum 1649 K after 20 minutes and remains same for 25 minutes and again starts reducing for 15 minutes. There are 10 similar temperature variation cycles in one day.

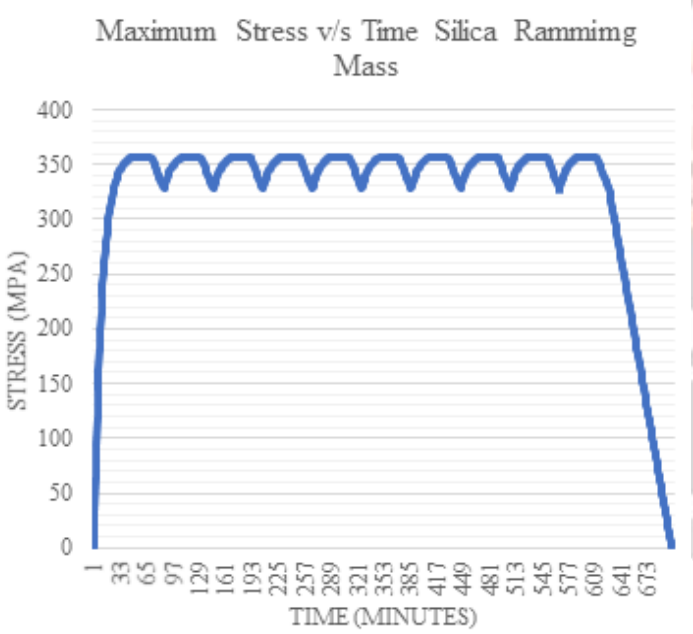

Figure 4 Maximum Thermal Stress v/s Time Plot for Silica Ramming Mass

It can be observed from the Figure 4 that maximum thermal stress for silica ramming mass is increasing from initial condition 0 MPa and reaches to maximum stress 356MPa in 45 minutes. Then it remains constant for 25 minutes and then starts reducing and reaches to 328 MPa in next 15 minutes. It again starts increasing and reaches to maximum stress 356 MPa after 20 minutes and remains same for 25 minutes again it starts reducing. There are 10 similar thermal stress variation cycles in one day.

6. RESULTS OF THERMAL FATIGUE BEHAVIOR OF ALUMINA RAMMING MASS

In Figure 5, Stress – Log N curve is plotted which is utilized for prediction of life cycle of induction furnace wall for alumina ramming mass as it is requirement of stress life methodology. Stress – Log N curve for alumina ramming mass is produced with the help of ultimate strength 500 MPa and endurance limit 75 MPa which is found using endurance modifying factors.Maximum stress created in the induction furnace refractory wall for alumina ramming mass is 345.75 MPa which is found from the output of computer program made to solve advanced mathematical model. We generate a horizontal line from 345.75 MPa and where it cut the Stress – Log N curve we take it in the vertical direction and found value of Log N as 2.54. From answer of Log N, we can find value of N equal to 347 reversible stress cycles. Thus, we can derive from Stress – Log N graph that life cycle of induction furnace refractory wall made up of alumina ramming mass is 347 stress cycles.

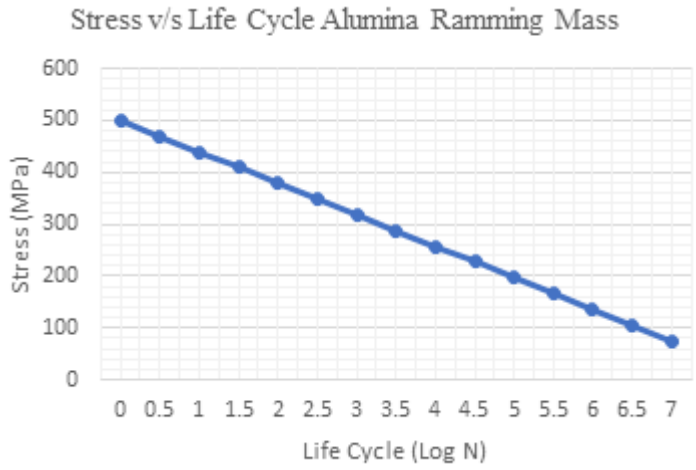

Figure 5 Stress v/s Life Cycle Graph for Alumina Ramming Mass

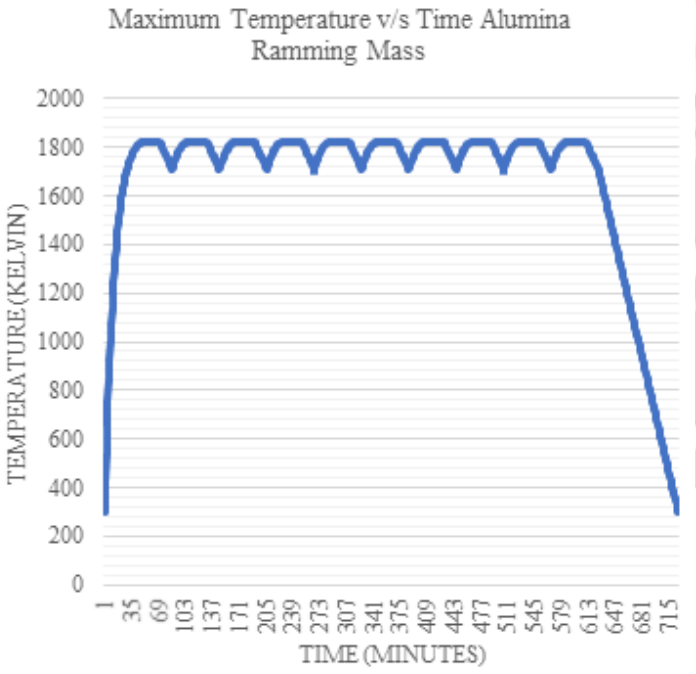

Figure 6 Maximum Temperature v/s Time Graph for Alumina Ramming Mass

It can be observed from the Figure 6 that maximum temperature for alumina ramming mass is increasing from atmospheric temperature 300 K and reaches to maximum temperature 1820 K in 45 minutes. Then it remains constant for 25 minutes and then starts reducing and reaches to 1709 K in next 15 minutes. It again starts increasing and reaches to maximum 1820 K after 20 minutes and remains same for 25 minutes and again starts reducing for 15 minutes. There are 10 similar temperature variation cycles in one day.

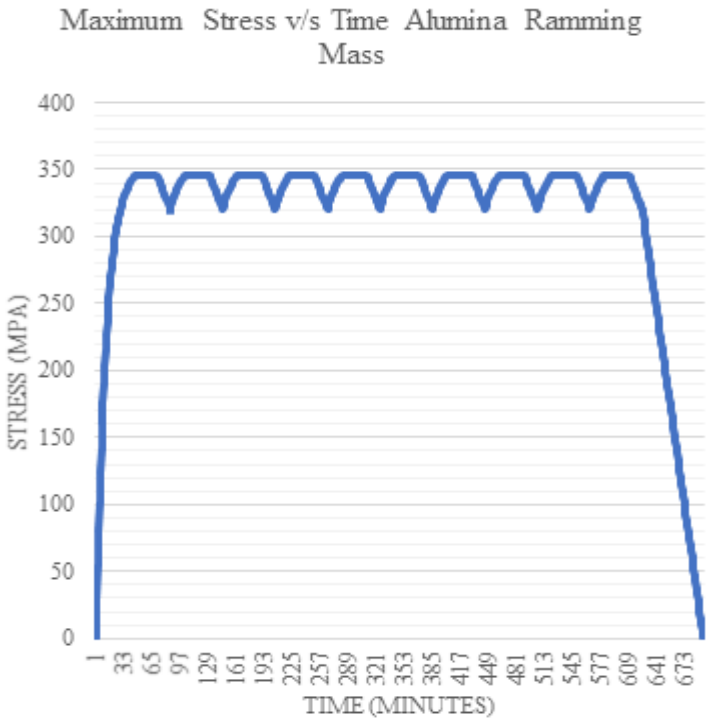

Figure 7 Maximum Thermal Stress v/s Time Plot for Alumina Ramming Mass

It can be observed from the Figure 7 that maximum thermal stress for alumina ramming mass is increasing from initial condition 0 MPa and reaches to maximum stress 345 MPa in 45 minutes. Then it remains constant for 25 minutes and then starts reducing and reaches to 320 MPa in next 15 minutes. It again starts increasing and reaches to maximum stress 345 MPa after 20 minutes and remains same for 25 minutes again it starts reducing. There are 10 similar thermal stress variation cycles in one day.

7. CONCLUSION

Induction melting furnaces are immensely used in modern era for melting of different kinds ofmaterials because of its advantages. The problem originates from the different refractory materials of losing its material properties and failure occurs within approximately 200-350 hours of life span. It will interrupt production schedule as it requires a lot of time to substitute the induction melting furnace wall. Explicit finite difference technique is utilized for finding temperature distribution and thermal stress distribution for induction melting furnace refractory wall and validation is done with respect to experimental outcomes. Explicit finite difference method is used with reference to actual working situations of induction furnace wall and physical properties of the varied refractory materials. Computer program is developed to resolve the mathematical model created by finite difference technique. Computer program uses stress life cycle methodology and it uses modified S – log N curves plotted for life cycle forecast. It is found approximately that life span for silica ramming mass is 233 cycles, alumina ramming mass is 347 cycles. From the comparison of experimental evaluations and finite difference investigation results for thermal fatigue failure of induction melting furnace wall, it can be detected that explicit finite difference model developed here can precisely predict the failure time of the induction furnace refractory wall and the positive solution conditions considered in the finite difference numerical calculations are approximately correct. The fatigue life cycle of the induction melting furnace refractory wall under thermal fatigue working conditions is predicted using stress-life technique by plotting modified S – log N curves for diverse materials on the foundation of explicit finite difference calculations and maximum thermal stress created in the induction melting furnace refractory wall by the support of advanced computer programming. The exactness of the fatigue life prediction for the induction melting furnace refractory wall depends upon temperature and thermal stress range calculated at the critical point by explicit finite difference technique and modified S-log N curves prepared from the material properties and boundary conditions for numerous ceramic based refractories.

REFERENCES

[1] D.M. Stefanescu, et al., (1992), Volume 15 Casting, ASM Handbook, ASM International Publication

[2] Barrie Jenkins and Peter Mullinger, (March 2008), Industrial and Process Furnaces,1st Edition, Butterworth-Heinemann Publication

[3] A V K Suryanarayana, (2005), Fuels Furnaces Refractory and Pyrometry, B S Publication

[4] J. Oh, U. Han, J. Park and H. Lee, (2018) Numerical Investigation on Energy Performance of Hot Stamping Furnace, Applied Thermal Engineering, Pages 1-52, doi: https://doi.org/10.1016/j.applthermaleng.2018.10.083

[5] R. S. S. Makia*, M. Fajara, J. Maletaskica, A. V. Gubarevicha, K. Yoshidaa, T. Yanoa, T. S. Suzukib and T. Uchikoshib, (2018), Evaluation of thermal shock fracture resistance of B4C/CNT composites with a high-frequency induction-heating furnace, Materials Today: Proceedings Issue 16, Pages 137–143.

[6] Piotr Bulińskia, Jacek Smolkaa, Grzegorz Siwiecc, Leszek Blachac, SławomirGolakb, Roman Przyłuckib, MichałPalacza and BartłomiejMelkaa, (2019), Numerical examination of the evaporation process within a vacuum induction furnace with a comparison to experimental results, Applied Thermal Engineering, Issue 150, Pages 348-358.doi: https://doi.org/10.1016/j.applthermaleng.2019.01.008

[7] Thomas J. Fleminga, Alan Kavanagha, Greg Duggana, Brian O'Mahonya and Mackenzie Higgensb, (2019), The effect of induction heating power on the microstructural and physical properties of investment cast ASTM-F75 CoCrMo alloy, Journal of Materials Research and Technology, Volume 8, Issue 5, Pages 4417-4424. doi: https://doi.org/10.1016/j.jmrt.2019.07.052

[8] Mochida, K. Kudo, Y. Mizutani, M. Hattorp And Y. Nakamura, (July–September 1997), Transient heat transfer analysis in vacuum furnaces heated by radiant tube burners, Energy Conservation and Management, Volume 38, Issue 10-13, Pages 1169–1176.

[9] E.P. Keramidaa, H.H. Liakosa, M.A. Fountib, A.G. Boudouvisa and N.C. Workatosa, (May 2000), Radiation heat transfer in natural gas-fired furnaces, International Journal of Heat and Mass Transfer, Volume 43, Issue 10, Pages 1801–1809.

[10] J.I. Ghojel, R.N. Ibrahim, (November 2004), Computer simulation of the thermal regime of double-loop channel induction furnaces, Journal of Materials Processing Technology, Volume 153-154, Pages 386–391.doi: 10.1016/j.jmatprotec.2004.04.123

[11] Man Young Kim, (September 2007), A heat transfer model for the analysis of transient heating of the slab in a direct-fired walking beam type reheating furnace, International Journal of Heat and Mass Transfer, Volume 50, Issue 19-20, Pages 3740–3748.doi:10.1016/j.ijheatmasstransfer.2007.02.023

[12] Stefan Murza, Björn Henning, Hans-Dieter Jasper, (November 2007), CFD-simulation of melting furnaces for secondary aluminium, Heat Processing, Volume 5, Issue 2, Pages 123-126.

[13] Yu Zhang, Rohit Deshpande, D. Frank Huang, PinakinChaubal, Chenn Zhou, (January 2008), Numerical analysis of blast furnace hearth inner profile by using CFD and heat transfer model for different time periods, International Journal of Heat and Mass Transfer, Volume 51, Issue 1-2, Pages 186–197.doi:10.1016/j.ijheatmasstransfer.2007.04.052

[14] A. Bermúdez, D. Gómez, M.C. Muñiz, P. Salgado, R. Vázquez, (2009), Numerical simulation of a thermo-electro magneto-hydrodynamic problem in an induction heating furnace, Applied Numerical Mathematics, Volume 59, Issue 1, Pages 2082–2104.doi:10.1016/j.apnum.2008.12.005

[15] M. M. Ahmed, M. Masoud, A. M. El-Sharkawy, (February 2009), Design of a Coreless Induction Furnace for Melting Iron, International Conference on Communication, Computer and Power, Pages 102-106.

[16] N. Depreea, J. Sneydb, S. Taylorb, M.P. Taylora, J. Chenc, S. Wangb, M. O' Connord, (January 2010), Development and validation of models for annealing furnace control from heat transfer fundamentals, Computers and Chemical Engineering, Elsevier, Volume 34, Issue 1, Pages 1849-1853.doi:10.1016/j.compchemeng.2010.01.012

[17] Xia Zhoua, ZhanfeiTanga, Guohui Qu, (April 2010), Thermal stress and thermal fatigue analysis of the continuous casting tundish cover, Material Science and Engineering, Volume 527, Issue 9, Pages 2327–2334.

[18] J. Govardhan, G.V.S. Rao, J. Narasaiah, (2011), Experimental investigations and CFD study of temperature distribution during oscillating combustion in a crucible furnace, International Journal of Energy and Environment, Volume 2, Issue 5, Pages 783-796.

[19] R. K. Jain, B. D. Gupta, (May 2011), Modelling and Optimisation of Flame Temperature in Rotary Furnace, Indian Foundry Journal, Volume 57, Issue 5, Pages 29-31.

[20] O.A. Ighodalo, (June 2011), Current Trend in Furnace Technology in the Melting Industries, Research Journal of Applied Sciences, Engineering and Technology, Volume 3, Issue 3, Pages 540-545.

[21] R. Comesaña, J. Porteiro, E. Granada, J.A. Vilán, M.A. Álvarez Feijoo, P. Eguía, (August 2011), CFD analysis of the modification of the furnace of a TG–FTIR facility to improve the correspondence between the emission and detection of gaseous species, Applied Energy, Volume 89, Pages 262-272.doi:10.1016/j.apenergy.2011.07.029

[22] A. Bhat, S. Agarwal, D. Sujish, B. Muralidharan, B.P. Reddy, G. Padmakumar, K.K. Rajan, (2012), Thermal Analysis of Induction Furnace, COSMOL Conference Bangalore

[23] Bhujbal Nitin B., Prof. S.B. Kumbhar, (April 2013), Optimization of Wall Thickness and Material for Minimum Heat Losses for Induction Furnace by FEA, International Journal of Mechanical Engineering and Technology, Volume 4, Issue 2, Pages 418-428.

[24] Nihar Bara, (May 2013), Review Paper on Numerical Analysis of Induction Furnace, International Journal of Latest Trends in Engineering and Technology, Volume 2, Issue 3, Pages 178-184.

[25] Nihar P Bara, (May 2013), Finite Element Analysis of Induction Furnace for Optimum Heat Transfer, International Journal of Innovative Research in Science, Engineering and Technology, Volume 2, Issue 5, Pages 1313-1319.

[26] R. Marigoudar, S.R. Patil, (2013), Role of Fatigue Life in industrial Designs, IOSR Journal of Mechanical and Civil Engineering, Second National Conference on Recent Developments in Mechanical Engineering, Pages 38-44.

[27] Richa Agrawal, Rashmi Uddanwadiker, Pramod Padole, (July 2014), Low Cycle Fatigue Life Prediction, International Journal of Emerging Engineering Research and Technology, Volume 2, Issue 4, Pages 5-15.

[28] Uma Kulkarni, Dr. Uday Wali, (February 2014), Design & Control of Medium Frequency Induction Furnace for Solar Grade Silicon, International Journal of Emerging Technology and Advanced Engineering, Volume 4, Special Issue 1, Pages 230-233.

[29] Sylvester Olanrewaju Omole, Raymond Taiwo Oluyori, (October 2014), Optimization of Recuperative System in Rotary Furnace for Minimization of Elemental Loss during Melting, Journal of Minerals and Materials Characterization and Engineering, Volume 2, Pages 579-585.

[30] Muhammad Mansoor, Muhammad Shahid, (2014), On the Designing, Efficiency, and Stirring Force of an Induction Coil for the Processing of Prototype Al Based Nanocomposites, Journal of Metallurgy, Volume 2, Pages-2-7. doi: http://dx.doi.org/10.1155/2014/637031

[31] Dharmendra K. Dodiya, Mr. Vasim G. Machhar, (2015), Optimization of Wall Thickness and Thermal Conductivity for Minimum Heat Losses for Induction Furnace by FEA, International Journal for Scientific Research & Development, Volume 3, Issue 3, Pages 589-596.

[32] Petrone G., Barbagallo C., Scionti M., (2015), Thermo-Mechanical Analysis and Fatigue Life Prediction for an Electronic Surface-Mount Device, Proceedings of the 2015 COMSOL Conference in Grenoble

[33] Bhaskar Dhiman, O.S. Bhatia, (August 2015), Oil Fired Furnace and Induction Furnace: A Review, International Journal of Scientific & Engineering Research, Volume 6, Issue 8, Pages 602-613.

[34] Amol V. Patil, S. G. Bhosale, (2016), Optimization of Wall Thickness for Minimum Heat Losses in an Induction Furnace, Journal of Material Science & Manufacturing Technology, Volume 1, Issue 1, Pages 1-15.

[35] V. Madhusudhan, S. DhivyaPriya, (2016), Wall Thickness Analysis in Induction Furnace for Optimum Heat Transfer Using ANSYS, International Conference on Breakthrough in Engineering, Science & Technology, Pages 55-61.

[36] Digvijay D. Patil, Prof. Dayanand A. Ghatge, (January 2017), Parametric Evaluation of Melting Practice on Induction Furnace to Improve Efficiency and System Productivity of CI and SGI Foundry-A Review, International Advanced Research Journal in Science, Engineering and Technology, Volume 4, Special Issue 1, Pages 160-163.doi: 10.17148/iarjset/ncdmete.2017.36

[37] Nilesh T. Mohite, Ravindra G. Benni, (2017), Optimization of Wall Thickness for Minimum Heat Losses for Induction Furnace, International Journal of Engineering Research and Technology, Volume 10, Issue 1, Pages 453-461.

[38] Yunus A. Cengel, (2012), Heat and Mass Transfer-A Practical Approach, McGraw Hill Publication

[39] Joseph E. Shigley and Charles R. Mischke, (2011), Machine Engineering Design, 9th Edition, Tata McGraw Hill Publication

[40] Nirajkumar C Mehta, Dr. C D Shankhavara, "CFD Analysis of Induction Furnace – Review", International Conference on Emerging Technologies and Applications in Engineering, Technology and Sciences, ISBN No. 978-81-906220-3-5, March 2012.

[41] Nirajkumar C Mehta, Akash D Raiyani, Vikash R Gondaliya, "Thermal Fatigue Analysis of Induction Melting Furnace for Silica Ramming Mass", International Journal of Emerging Technology and Advanced Engineering, ISSN No. 2250-2459, Volume 3, Issue 2, pp 357-362, February 2013.

[42] Nirajkumar C Mehta, Vipul B Gondaliya, Jayesh V Gundania, "Application of Different Numerical Methods in Heat Transfer - A Review", International Journal of Emerging Technology and Advanced Engineering, ISSN No. 2250-2459, Volume 3, Issue 2, pp 363-368, February 2013.

[43] Vimal R Nakum, Kevin M Vyas, Nirajkumar C Mehta, "Research on Induction Furnace – Review", International Journal of Science and Engineering Applications, ISSN No. 2319-7560, Volume 2, Issue 6, pp 141-144, April 2013.

[44] Nirajkumar C Mehta, Viral V Shiyani, Jemish R Nasit, “Metal Forming Analysis”, International Journal of Emerging Technology and Advanced Engineering, ISSN No. 2250-2459, Volume 3, Issue 5, pp 190-196, May 2013.

[45] Vipul Gondaliya, Mehul Pujara, Nirajkumar C Mehta, "Transient Heat Transfer Analysis of Induction Furnace by Using Finite Element Analysis", International Journal of Applied Research, ISSN No. 2249-555X, Volume 3, Issue 8, pp 231-234, August 2013.

[46] Nirajkumar C Mehta, Vasim G Machhar, Ravi K Popat, "Thermal Fatigue Analysis of Induction Furnace Wall for Alumina Ramming Mass", International Journal of Science and Engineering Applications, ISSN No. 2319-7560, Volume 2, Issue 10, pp 186-190, October 2013.

[47] Akash D. Raiyani, N. R. Sheth, Nirajkumar C Mehta, "Thermal Analysis of Hot Wall Condenser for Domestic Refrigerator", International Journal of Science and Research, ISSN No. 2319-7064, Volume 3, Issue 7, pp 622-626, July 2014.

[48] Nirajkumar C Mehta, Dipesh D Shukla, Ravi K Popat, "Optimization of Wall Thickness for Minimum Heat Loss for Induction Furnace by FEA", Indian Foundry Journal, ISSN No. 0379-5446, Volume 60, Issue 12, pp 19-25, December 2014.

[49] Nirajkumar C Mehta, Dr. Dipesh D Shukla, Pragnesh D Kandoliya, “Comparison of Finite Difference Method and Finite Element Method for 2 D Transient Heat Transfer Problem”, National Conference on Recent Research and Development in Core Disciplines of Engineering, Vadodara, Volume: 2, April 2015.

[50] Nirajkumar C Mehta, Dr. Dipesh D Shukla, Vishvash B Rajyaguru, “Numerical Analysis of Furnace: Review”, National Conference on Recent Research and Development in Core Disciplines of Engineering, Vadodara, Volume: 2, April 2015.

[51] Nirajkumar C Mehta, Dr. Dipesh D Shukla, Vishvash B Rajyaguru, “Thermal Fatigue Analysis of Induction Furnace Wall for Zirconia”, National Conference on Recent Research and Development in Core Disciplines of Engineering, Vadodara, Volume: 2, April 2015.

[52] Nirajkumar C Mehta, Dr. Dipesh D Shukla, “Thermal Fatigue Analysis of Induction Furnace Wall for Magnesia Ramming Mass”, ASME 2015 Applied Mechanics and Materials Conference, At Seattle, Washington, United States of America, June 2015.

[53] Pragnesh D Kandolia, Nirajkumar C Mehta, “A Recent Review of Refrigerant R-1234yf and R-1234ze (E)”, International Journal of Recent Scientific Research, ISSN No. 2349-5162, Volume 3, Issue 11, pp 59-64, November 2016.

[54] Nirajkumar C Mehta, Dr. Dipesh D Shukla, Pragnesh D Kundalia, “Advanced Mathematical Modelling of Heat Transfer in Induction Furnace Wall of Zirconia”, International Journal of Engineering Research & Technology, ISSN No. 2278-0181, Volume 5, Issue 12, pp 176-181, December 2016.

[55] Nirajkumar C Mehta, Dr. Dipesh D Shukla, Pragnesh D Kundalia, “Advanced Heat Transfer Analysis of Alumina Based Refractory Wall of Induction Furnace”, National Conference on "Emerging Trends in Engineering", ISBN No. 978-93-84659-91-2, At Tolani Polytechnic, Adipur, Volume: 1, December 2016.

[56] Nirajkumar C Mehta, Dr. Dipesh D Shukla, “Prediction of Life Cycle of Induction Furnace Wall for Silica Ramming Mass”, International Journal of Thermal Technologies, ISSN No. 2277-4114, Volume 6 Issue 4, pp 364-372, December 2016.

[57] Nirajkumar C Mehta, Dr. Dipesh D Shukla, “Finite Difference Analysis of Induction Furnace Wall for Magnesia Ramming Mass”, SSRG International Journal of Thermal Engineering, ISSN No. 2395-0250, Volume 3, Issue 1, pp 1-7, January 2017.

[58] Nirajkumar C Mehta, Dr. Dipesh D Shukla, “Computational Investigation of Furnace Wall for Silica Ramming Mass with FDM”, International Journal of Advanced Engineering Research and Science, ISSN No. 2456-1908, Volume 4, Issue 2, pp 133-139, February 2017.

[59] Nirajkumar C Mehta, Dr. Dipesh D Shukla, “Stress Life Analysis of Induction Furnace Wall for Magnesia Ramming Mass”, IOSR Journal of Mechanical and Civil Engineering, e-ISSN: 2278-1684, p-ISSN: 2320-334X, Volume 14, Issue 1, pp 60-70, February 2017.

[60] Kaushik Parmar, Osama Gora, Kashyap Desai, Nirajkumar C Mehta, “A Practical Attempt to Improve Performance of Heat Exchanger”, International Journal of Advance Research and Innovative Ideas in Education, ISSN 2395-4396, Volume 3, Issue 1, March 2017.

[61] Nirajkumar C Mehta, Dr. Dipesh D Shukla, “Mathematical Modelling for Life Cycle Forecasting of Zirconia Based Furnace Wall”, International Journal of Advance Research and Innovative Ideas in Education, ISSN 2395-4396, Volume 3, Issue 4, April 2017.

[62] Nirajkumar C Mehta, Dr. Dipesh D Shukla, Comparison of Life Cycle for Various Refractory Materials of Induction Melting Furnace Wall under Thermal Fatigue Loading Conditions”, International Journal of Advance Engineering and Research Development, e-ISSN (O): 2348-4470, p-ISSN (P): 2348-6406, Volume 5, Issue 01, January -2018.

[63] Patil Kaushal, Makwana Arjunsinh, Arab Mohammadazhar, Nirajkumar C Mehta, "Mathematically Advanced Computational Heat Transfer Analysis of Cylindrical and Spherical Induction Furnaces: Review", International Journal of Advance Engineering and Research Development, e-ISSN (O): 2348-4470, p-ISSN (P): 2348-6406, Volume 5, Issue 02, February -2018.

[64] Ronik Varia, Sachin Vasani, Rahul Varma, Dr. Nirajkumar C Mehta, "Review of Solar Heating Furnace Development", International Journal of Advance Engineering and Research Development, e-ISSN (O): 2348-4470, p-ISSN (P): 2348-6406, Volume 5, Issue 03, March -2018.

[65] Rahul Waghela, Shreyas Parmar, Susmit Vasava, Dr. Nirajkumar C Mehta, "Review of Refractory Materials for Innovative Investigation and Testing", International Journal of Advance Engineering and Research Development, e-ISSN (O): 2348-4470, p-ISSN (P): 2348-6406, Volume 5, Issue 03, March -2018.